

# AX J1910.7+0917: the slowest X–ray pulsar

L. Sidoli,<sup>1\*</sup> G. L. Israel,<sup>2</sup> P. Esposito,<sup>3</sup> G. A. Rodríguez Castillo,<sup>2</sup> and K. Postnov<sup>4,5</sup>

<sup>1</sup>INAF, Istituto di Astrofisica Spaziale e Fisica Cosmica, Via E. Bassini 15, I-20133 Milano, Italy

<sup>2</sup>INAF, Osservatorio Astronomico di Roma, Via Frascati 33, I-00040 Monteporzio Catone, Italy

<sup>3</sup>Anton Pannekoek Institute for Astronomy, University of Amsterdam, Postbus 94249, NL-1090-GE Amsterdam, The Netherlands

<sup>4</sup>Moscow Lomonosov State University, Faculty of Physics, Leninskie Gory 1/2, 119991, Moscow Russia

<sup>5</sup>Moscow Lomonosov State University, Sternberg Astronomical Institute 13, Universitetskij pr., 119234, Moscow, Russia

Accepted 2017 May 3. Received 2017 May 3; in original form 2017 April 6

## ABSTRACT

Pulsations from the high mass X-ray binary AX J1910.7+0917 were discovered during *Chandra* observations performed in 2011 (Israel et al. 2016). We report here more details on this discovery and discuss the source nature. The period of the X-ray signal is  $P = 36200 \pm 110$  s, with a pulsed fraction,  $PF$ , of  $63 \pm 4\%$ . Given the association with a massive B-type companion star, we ascribe this long periodicity to the rotation of the neutron star, making AX J1910.7+0917 the slowest known X–ray pulsar. We report also on the spectroscopy of *XMM-Newton* observations that serendipitously covered the source field, resulting in an highly absorbed (column density almost reaching  $10^{23}$  cm<sup>-2</sup>), power law X-ray spectrum. The X-ray flux is variable on a timescale of years, spanning a dynamic range  $\gtrsim 60$ . The very long neutron star spin period can be explained within a quasi-spherical settling accretion model, that applies to low luminosity, wind-fed, X–ray pulsars.

**Key words:** accretion - stars: neutron - X–rays: binaries - X–rays: individual (AX J1910.7+0917, CXOU J191043.7+091629, 2XMM J191043.4+091629)

## 1 INTRODUCTION

AX J1910.7+0917 (also known as 2XMM J191043.4+091629) was discovered during the ASCA Galactic Plane Survey and it was included in the catalogue of the faint point-like sources (Sugizaki et al. 2001). Different X–ray missions serendipitously covered the source position, since it lies at a projected distance of about 12' from the Supernova Remnant (SNR) W49, target of many observations.

Pavan et al. (2011) performed a comprehensive investigation of all X–ray data that were publicly available at that time, analysing ASCA (performed in 1993), *XMM-Newton* (2004) and *Chandra* observations (2008), finding that AX J1910.7+0917 is a variable (maybe transient) X-ray source. No periodicities in the X–ray light curves were found. Their X–ray spectroscopy resulted in a highly absorbed power law spectrum, well described by a column density,  $N_{\text{H}}$ , of a few  $10^{22}$  cm<sup>-2</sup>, and a photon index ranging from  $\Gamma=2.3 \pm 0.5$  (at a 1–10 keV observed flux of  $\sim 5 \times 10^{-12}$  erg cm<sup>-2</sup> s<sup>-1</sup>; ASCA) to  $\Gamma=1.28 \pm 0.08$  (at a 1–10 keV observed flux of  $2.4 \times 10^{-11}$  erg cm<sup>-2</sup> s<sup>-1</sup>; *XMM-Newton*). A faint emission line from iron at  $\sim 6.4$  keV was also evident in the *XMM-Newton* 2004 spectra. During the only available *Chandra* observation pointed on AX J1910.7+0917 the source was undetected, with

a 1–10 keV flux  $F < 4 \times 10^{-13}$  erg cm<sup>-2</sup> s<sup>-1</sup> ( $1\sigma$  upper limit; not corrected for the absorption; Pavan et al. 2011).

A refined X–ray position with respect to the ASCA survey could be estimated from *XMM-Newton*/EPIC data (where the source was caught at large off-axis angle; Pavan et al. 2011): R.A.<sub>J2000</sub>=19<sup>h</sup>10<sup>m</sup>43<sup>s</sup>.39, Dec<sub>J2000</sub>=09°16'30".0, with an uncertainty of 2" (90% c.l.). Using these sky coordinates, a 2MASS counterpart was at first associated with AX J1910.7+0917 (Pavan et al. 2011), favouring a high mass X-ray binary (HMXB) nature. Later, this infrared (IR) source was resolved into two stars by Rodes-Roca et al. (2013) using the UKIDSS-GPS (United Kingdom Infrared Deep Sky Survey-Galactic Plane Survey; Lucas et al. 2008). Only one of these two stars lies within the XMM error region. The near-infrared (NIR) spectrum of this counterpart, obtained with the Near-Infrared Camera Spectrometer (NICS) at the Telescopio Nazionale *Galileo* (TNG) allowed them to identify it with a B-type star, confirming a massive binary nature for AX J1910.7+0917 (Rodes-Roca et al. 2013), although the luminosity class (a supergiant or a Be star) could not be securely established. However, these authors favoured a supergiant HMXB located at a distance  $d=16.0 \pm 0.5$  kpc, following a comprehensive discussion of both X-ray and NIR properties.

AX J1910.7+0917 is also reported at hard energies (above 20 keV) as a variable HMXB in the *INTEGRAL*/IBIS source catalog (Bird et al. 2016).

During a systematic search for coherent signals in publicly

\* E-mail: sidoli@iasf-milano.inaf.it

available *Chandra* observations, a periodicity at 36.2 ks was found from a faint source (named CXOU J191043.7+091629) compatible with being AX J1910.7+0917 (Israel et al. 2016).

In this *paper*, we give details on this discovery and discuss the source nature.

## 2 OBSERVATIONS AND DATA REDUCTION

The CXOU J191043.7+091629 sky position was serendipitously observed by *Chandra* and *XMM-Newton*, during observations pointed on the SNR W49. The results on the SNR were published by Lopez et al. (2013) and Miceli et al. (2006). Results on some archival X-ray data of AX J1910.7+0917 were reported by Pavan et al. (2011), to which we refer the reader. We have analysed more recent *XMM-Newton* and *Chandra* long exposures of the source field, summarized in Table 1.

During the two long *Chandra*/Advanced CCD Imaging Spectrometer (ACIS; Garmire et al. 2003) observations performed in 2011 the source was located in one of the two ACIS-I, front-illuminated CCDs, operated in full-imaging timed-exposure mode (no gratings) and with a frame time of 3.24 s. New level 2 event files were generated with the *Chandra* Interactive Analysis of Observations (CIAO) software version 4.8, and products extracted adopting standard procedures. We refer the reader to Israel et al. (2016) for additional details on the data reduction not contained in this paper.

The source field was covered by *XMM-Newton*/EPIC (European Photon Imaging Camera) detectors, two of which use MOS CCDs (Turner et al. 2001) while the third uses pn CCDs (Strüder et al. 2001). Due to the loss of one EPIC-MOS CCD (caused by a micro-meteorite<sup>1</sup>), the AX J1910.7+0917 off-axis position was imaged in 2014 only by MOS 2 and pn CCDs (Table 1), both operated in full frame mode. The data were reprocessed using version 15 of the Science Analysis Software (SAS) with standard procedures. Background counts were obtained from regions offset from the source position on the same CCD, at a similar off-axis distance. The background level was stable along the observations, except than during the 2014 *XMM-Newton* pointings, where a further filtering was applied to exclude time intervals containing background flares. This led to reduced net exposure times of 98.2 ks (pn) and 109.4 ks (MOS 2) for the 0724270101 observation, and of 30.8 ks (pn) and 34.7 ks (MOS 2) for the 0724270201 one. Appropriate response matrices were generated using the SAS tasks ARFGEN and RMFGEN.

For both *XMM-Newton* and *Chandra* spectra, all uncertainties are given at 90% confidence level for one interesting parameter. Spectra were grouped to have a minimum of 30 counts per bin. When fitting two EPIC spectra from a single observation, we fitted them simultaneously, adopting normalization factors to account for uncertainties in instrumental responses. In the spectral fitting we adopted the interstellar abundances of Wilms et al. (2000) and photoelectric absorption cross-sections of Verner et al. (1996), using the absorption model TBNEW in XSPEC.

Arrival times have been corrected to the Solar System barycenter before searching for periodicities.

## 3 ANALYSIS AND RESULTS

### 3.1 X-ray position

AX J1910.7+0917 is located at a very large off-axis position in the X-ray observations analysed in this paper (Fig. 1), so unfortunately we are unable to provide refined X-ray sky coordinates, with respect to Pavan et al. (2011). The sky position we estimated from the *Chandra* observations is  $R.A._{J2000}=19^{\text{h}}10^{\text{m}}43^{\text{s}}.6$ ,  $Dec_{J2000}=09^{\circ}16'28''.9$  (J2000), with an associated  $1\sigma$  error of  $7''$ . The big error region is due to the large off-axis source position (Evans et al. 2010). The *Chandra* centroid is  $\sim 3.3''$  away from the XMM one (Pavan et al. 2011), and is compatible with the infrared counterpart proposed by Rodes-Roca et al. (2013), an early-type massive companion.

### 3.2 Timing analysis

As part of the *Chandra* ACIS Timing Survey (CATS; Israel et al. 2016) project,<sup>2</sup> a coherent signal with a period of 36.2 ks was discovered from AX J1910.7+0917. The Fourier periodogram (normalized according to Leahy et al. 1983) is shown in Fig. 2 (left panel) together with the net light curve (right panel) fitted with a sinusoidal model. The periodic modulation is clearly evident, as well as a variability of the peak intensity at each cycle. Adopting a phase-fitting technique (Dall’Osso et al. 2003) using three time intervals, we estimated a final value for the periodicity of  $P = 36200 \pm 110$  s ( $1\sigma$ ), obtaining a pulsed fraction (semi-amplitude of the sinusoid divided by the source average count rate) of  $PF=63\pm 4\%$  ( $1\sigma$ ).

The timing analysis of the *XMM-Newton* data did not provide any additional significant information about the periodic pulsation. The inspection of the longest observation (0724270101) revealed a possible modulation at  $\sim 9.5$  h. However, while the period is consistent with the *Chandra* one ( $P_{XMM} = 34200 \pm 2200$  s at  $3\sigma$ ), the signal is not statistically significant (we estimate a significance of  $\approx 3\sigma$ ); in this respect, we also note that in the *XMM-Newton* data set the upper limit on the pulsed fraction for a modulation around 36 ks is larger than 100% (as inferred from the PDS within a narrow frequency interval encompassing frequencies around the *Chandra* period) and therefore a non-detection would not be surprising. The successive *XMM-Newton* observation (0724270201) covered less than two modulation cycles and was affected by episodes of strong flaring background that hampered a proper search for periodicities.

### 3.3 Spectroscopy

We performed the spectroscopy of *Chandra* and *XMM-Newton* data adopting a simple, highly absorbed power law, which already resulted in a good deconvolution of the X-ray emission. The time-averaged spectral results for the five observations are reported in Table 2. While the absorbing column density is consistent with a constant value, the spectrum becomes harder when the source intensity is brighter. The source X-ray flux spans a dynamic range of  $\sim 60$ . The luminosity, calculated assuming a distance of 16 kpc (Rodes-Roca et al. 2013), ranges from  $1.7 \times 10^{34}$  erg  $s^{-1}$  to  $10^{36}$  erg  $s^{-1}$ . The uncertainty on the X-ray luminosity in Table 2 includes only the error on the power law normalization.

<sup>2</sup> The CATS project is a Fourier-transform-based systematic and automatic search for new pulsating sources in the *Chandra* ACIS public archive, yielding, to date, up to 41 previously unknown X-ray pulsators.

<sup>1</sup> see <https://www.cosmos.esa.int/web/xmm-newton/mos1-ccd3>

**Table 1.** Summary of the X-ray observations.

| Satellite      | Instrument    | Obs. ID    | Date        | Exp. (ks)     | Mode <sup>a</sup>         |
|----------------|---------------|------------|-------------|---------------|---------------------------|
| <i>Chandra</i> | ACIS          | 13440      | 2011 Aug 18 | 160.0         | TE FAINT (3.24 s)         |
| <i>Chandra</i> | ACIS          | 13441      | 2011 Aug 21 | 60.5          | TE FAINT (3.24 s)         |
| <i>XMM</i>     | MOS 1 / MOS 2 | 0084100601 | 2004 Apr 13 | 2.5 / 2.5     | FF (2.6 s) / FF (2.6 s)   |
| <i>XMM</i>     | pn / MOS 2    | 0724270101 | 2014 Apr 17 | 115.3 / 116.8 | FF (73.4 ms) / FF (2.6 s) |
| <i>XMM</i>     | pn / MOS 2    | 0724270201 | 2014 Apr 19 | 67.4 / 69.8   | FF (73.4 ms) / FF (2.6 s) |

<sup>a</sup> TE: Timed Exposure, FAINT: Faint telemetry format, FF: Full Frame, the readout time is given in parentheses.

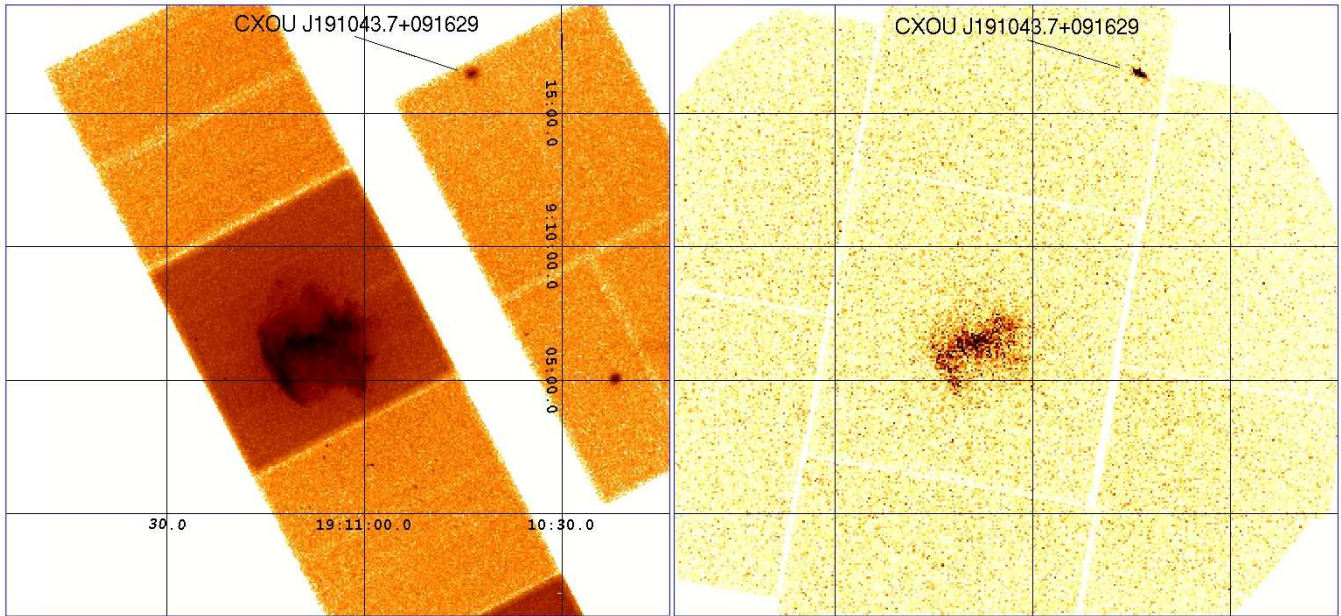


**Figure 1.** CXOU J191043.7+091629 sky position serendipitously observed by *Chandra* (on the left, obsID 13441) and by *XMM-Newton* (on the right, MOS 1, obsID 0084100601). The same scale applies to both images. The target was the SNR W49.

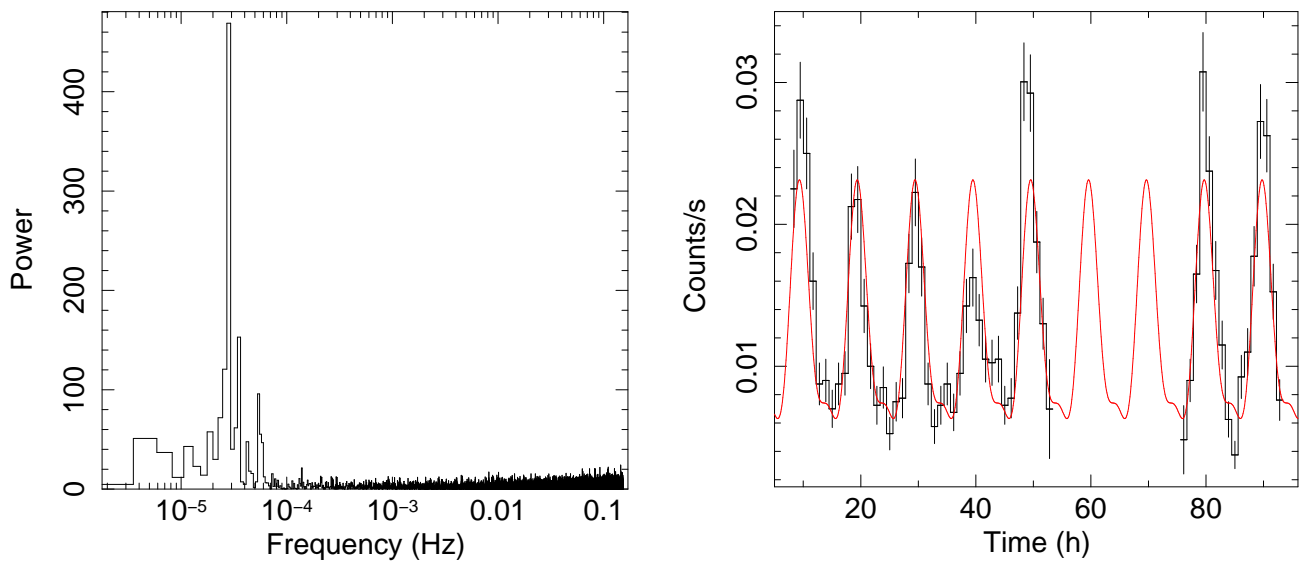


**Figure 2.** Power density spectrum (PDS) obtained from the *Chandra*/ACIS data (Left panel) together with the *Chandra* source light curve fitted with a sinusoidal model (Right panel).

Alternatively, a single absorbed hot blackbody model results in an equally good fit to the *Chandra* and 2014 *XMM-Newton* spectra, implying a lower column density,  $N_{\text{H}}$  in the range  $2\text{--}6 \times 10^{22} \text{ cm}^{-2}$ , a temperature  $kT_{\text{BB}} \sim 1.1\text{--}1.9 \text{ keV}$ , and blackbody radii in the range  $R_{\text{BB}} \sim 100\text{--}300 \text{ m}$  (at 16 kpc). More complicated models are not required by the data.

In Fig. 3 we show the long-term AX J1910.7+0917 light curve, plotting the observed X-ray flux (not corrected for the absorption), in the energy range 1–10 keV. We rely on Pavan et al. (2011) for AX J1910.7+0917 X-ray fluxes before 2004. All fluxes assume a power law continuum.

## 4 DISCUSSION

A coherent signal at 36.2 ks from the source CXOU J191043.7+091629 (AX J1910.7+0917) was discovered during long *Chandra* observations performed in 2011 (Israel et al. 2016). We have reported here details on this discovery, together with X-ray spectroscopy of more recent *XMM-Newton* pointings that serendipitously covered the source field.

AX J1910.7+0917 is a faint X-ray source the nature of which was previously investigated in depth by Pavan et al. (2011) and by Rodes-Roca et al. (2013). The latter authors performed a search for NIR counterparts, pinpointing a single early-B massive star within the *XMM-Newton* error circle provided by Pavan et al. (2011). Although Rodes-Roca et al. (2013) could not constrain the luminosity class of the B-type star, being consistent with both a supergiant and a main sequence, Be star, they favoured a supergiant HMXB located at a distance of  $16.0 \pm 0.5 \text{ kpc}$ , in the Outer Arm of our Galaxy. Since AX J1910.7+0917 was always detected at very large offaxis angles also in the more recent X-ray data-set analysed in our work, we are unable to provide better sky coordinates (Sect. 3.1) than the one already reported by Pavan et al. (2011). So we rely on these two previous papers for the source nature, where compelling evidence of an HMXB nature was found.

The X-ray properties we observed from the source in our data-set are consistent with a HMXB nature as well: the long-term X-ray light curve (Fig. 3) displays a dynamic range larger than 60, with an X-ray luminosity (at a distance of 16 kpc, Rodes-Roca et al. (2013)), ranging from  $1.7 \times 10^{34} \text{ erg s}^{-1}$  to  $10^{36} \text{ erg s}^{-1}$ ; the X-ray emission is well characterized by a highly absorbed power-law model, harder (in the range 1–10 keV) when the source is brighter, in agreement with what usually found in HMXB pulsars (see Walter et al. 2015 and Martínez-Núñez et al. 2017, for the most recent reviews on HMXBs).

Given the well-ascertained HMXB nature, the only viable interpretation of the  $\sim 10 \text{ hr}$  coherent signal is that it is the rotational period of the neutron star, making AX J1910.7+0917 the slowest X-ray pulsar known to date. Indeed, before AX J1910.7+0917, the slowest X-ray pulsar in an HMXB was 2S 0114+650 (associated with a B1Ia donor; Grundstrom et al. 2007), with a periodicity of  $\sim 2.7 \text{ hr}$  (Finley et al. 1992; Hall et al. 2000; Hu et al. 2016). A slowly rotating neutron star with a period of  $\simeq 5.3 \text{ hr}$  was also detected in a symbiotic X-ray binary with red giant donor 3A 1954+319 (Marcu et al. 2011), while an isolated pulsar with a very long spin period of 6.67 hr was discovered within the supernova remnant RCW 103 (De Luca et al. 2006).

### 4.1 Quasi-spherical settling accretion

The very slow period of the observed X-ray flux can be the spin period of a neutron star (NS) at the stage of quasi-spherical settling accretion in a wind-fed HMXB. This stage of accretion onto magnetized NS can be established when the X-ray luminosity of the source falls below some critical value  $L_x \lesssim 4 \times 10^{36} \text{ erg s}^{-1}$  (Shakura et al. 2012; see also Shakura & Postnov 2017 for a recent update). In this regime, the accreting matter entry rate into NS magnetosphere, which determines the X-ray luminosity from the NS ( $L_x \simeq 0.1 \dot{M} c^2$ ), is controlled by the plasma cooling due to Compton processes (at luminosities roughly above  $10^{35} \text{ erg s}^{-1}$ ) or radiative plasma cooling at lower luminosities. In a binary system with the orbital period  $P_b = 2\pi/\omega_B$ , the torques acting on a magnetized NS rotating with the period  $P^* = 2\pi/\omega^*$  read:

$$I\dot{\omega}^* = Z\dot{M}\omega_B R_B^2 - Z(1-z/Z)\dot{M}R_A^2\omega^*, \quad (1)$$

where  $I = 10^{45} \text{ g cm}^2$  is the NS moment of inertia,  $Z > 1$  is the dimensionless coupling coefficient between plasma and the NS magnetosphere (determined by the plasma cooling efficiency),  $z \lesssim 1$  is the dimensionless factor describing the specific angular momentum of matter brought to the NS surface by accreting matter,  $R_B = 2GM_x/v_w^2$  is the gravitational capture (Bondi) radius of the NS from the stellar wind with the relative velocity  $v_w$ ,  $M_x$  is the NS mass, and  $R_A$  is the Alfvén magnetospheric radius, which is determined by the pressure balance of matter near the magnetospheric boundary. This equation can be conveniently recast to the relaxation form:

$$\dot{\omega}^* = \frac{1}{\tau}(\omega_{eq}^* - \omega^*) \quad (2)$$

where  $\omega_{eq}^* = (1-z/Z)^{-1}\omega_B(R_B/R_A)^2$  is the equilibrium NS frequency found from the vanishing torque condition  $\dot{\omega}^* = 0$ , and  $\tau$  is the characteristic time of reaching the equilibrium:

$$\tau = \frac{I}{Z\dot{M}(1-z/Z)R_A^2}. \quad (3)$$

For the characteristic values  $\dot{M} = 10^{14} \text{ g s}^{-1}$  (corresponding to the X-ray luminosity  $L_x = 10^{34} \text{ erg s}^{-1}$ ) and the canonical NS surface magnetic field  $B = 10^{12} \text{ G}$  (corresponding to the NS dipole magnetic moment  $\mu = 10^{30} \text{ G cm}^3 \mu_{30}$ ), we find (see Shakura & Postnov 2017 for more detail and derivations) that the magnetospheric radius is  $R_A \sim 3 \times 10^9 \text{ cm}$ ,  $Z \sim 5 - 10$  and  $\tau \simeq 10^4 \text{ years}$ , the latter being only weakly dependent on the mass accretion rate  $\dot{M}$ . The solution of Eq. 2 reads:  $\omega^*(t) = \omega_0^* e^{-t/\tau} + \omega_{eq}^*(1 - e^{-t/\tau})$ , where  $\omega_0^*$  is the initial NS spin frequency. Even if  $\omega_0^* \gg \omega_{eq}^*$ , the NS frequency  $\omega^*(t)$  tends to  $\omega_{eq}^*$  in several  $\tau$  intervals.

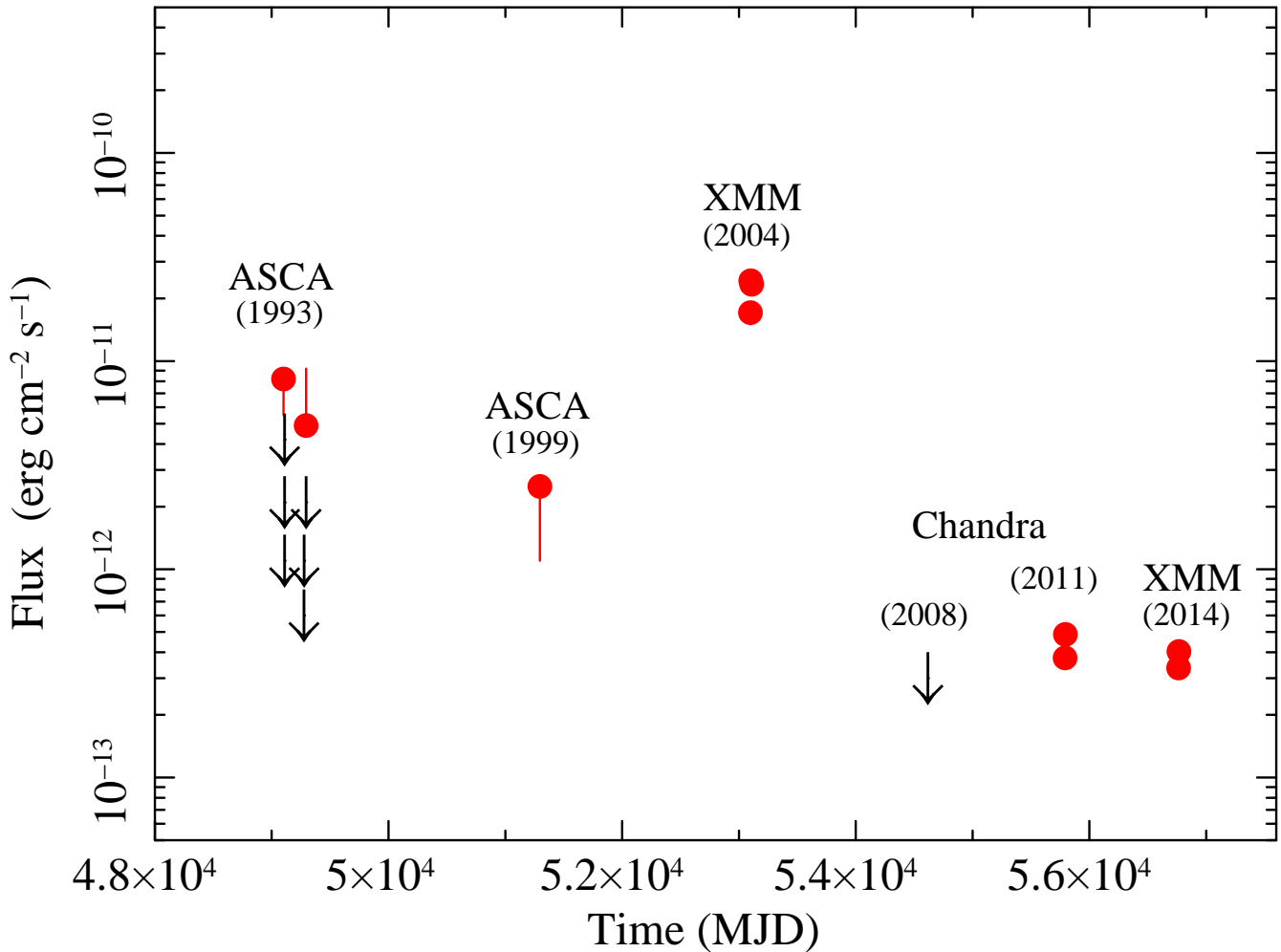
The short relaxation time  $\tau \sim 10^4 \text{ years}$  (keeping all the external parameters constant) suggests that in this accretion regime the NS rotation rapidly reaches the equilibrium period  $P_{eq}^* = 2\pi/\omega_{eq}^*$ :

$$P_{eq} \approx 5340 \text{ s } \mu_{30}^{12/11} \left( \frac{P_b}{10 \text{ d}} \right) \dot{M}_{14}^{-4/11} \left( \frac{v_w}{1000 \text{ km s}^{-1}} \right)^4. \quad (4)$$

This formula immediately suggests that to observe  $P_{eq} \approx 36200 \text{ s}$ , if we assume the standard NS magnetic field and the typical stellar wind velocity about  $1000 \text{ km s}^{-1}$ , the binary system should have an orbital period of about 68 days, which is longer than typical orbital periods of supergiant HMXBs (usually,  $P_b \sim 10 \text{ days}$ , Liu et al. (2006), but note that a large scatter is present and some outliers exist, like XTE J1739-302, with  $P_b = 51 \text{ days}$ , Drave et al. (2010), and IGRJ 11215-5952, with  $P_b = 165 \text{ days}$ , Sidoli et al. (2007)). However, increasing the NS magnetic field would decrease the orbital

**Table 2.** *Chandra* and *XMM-Newton* spectroscopy with an absorbed power law model.

| Obs.                   | $N_{\text{H}}$<br>( $10^{22} \text{ cm}^{-2}$ ) | $\Gamma$            | Unabs. flux (1-10 keV)<br>( $10^{-12} \text{ erg cm}^{-2} \text{ s}^{-1}$ ) | $L_X$ (1-10 keV)<br>( $10^{34} \text{ erg s}^{-1}$ ) | $\chi^2_{\nu} / \text{dof}$ |
|------------------------|---|---------------------|---|--|-----------------------------|
| <i>Chandra</i> /13440  | $10^{+2}_{-1}$                                  | $2.3 \pm 0.3$       | $0.99 \pm 0.05$   | $3.0 \pm 0.1$  | 0.814 / 109                 |
| <i>Chandra</i> /13441  | $9 \pm 2$                                       | $2.0^{+0.5}_{-0.4}$ | $1.07 \pm 0.07$   | $3.3 \pm 0.2$  | 0.884 / 51                  |
| <i>XMM</i> /0084100601 | $7^{+3}_{-2}$                                   | $0.9^{+0.5}_{-0.4}$ | $33 \pm 2$  | $100 \pm 7$  | 1.246 / 47                  |
| <i>XMM</i> /0724270101 | $8 \pm 2$                                       | $1.5^{+0.3}_{-0.3}$ | $0.57 \pm 0.03$   | $1.7 \pm 0.1$  | 1.114 / 58                  |
| <i>XMM</i> /0724270201 | $8^{+4}_{-3}$                                   | $1.5^{+0.6}_{-0.5}$ | $0.69 \pm 0.08$   | $2.1 \pm 0.2$  | 0.978 / 20                  |


**Figure 3.** AX J1910.7+0917 long-term light curve. Observed (not corrected for the absorption) X-ray fluxes in the energy range 1–10 keV have been collected from Pavan et al. 2011 and from the *present work*. When the error bars are not evident, they are smaller than the symbols.

period estimate,  $P_b \propto \mu^{-12/11}$ , and moderate increase in the NS magnetic field by a few times is already sufficient to explain the observed 36.2 ks spin period of the X-ray pulsar in AX J1910.7+0917 for more typical orbital periods of HMXBs with supergiants.

It is also easy to check that the mean X-ray luminosity  $10^{34} - 10^{35} \text{ erg s}^{-1}$  can be obtained assuming the typical values of the optical component mass  $10M_{\odot}$  and using the straightforward estimate of the captured wind rate by the NS in a HMXB [see Eq. (4) in Shakura et al. 2014]. Note, however, variable properties of the stellar wind can render settling accretion onto NS highly unstable, with sudden flares and outbursts of different amplitudes, as discussed for example in Shakura et al. (2014) in the context of Supergiant Fast

X-ray Transient (SFXT) sources. It would be interesting to monitor the long-term X-ray flux variability of this source which may share some of SFXT properties.

Therefore, the quasi-spherical settling accretion model for AX J1910.7+0917 naturally provides explanation to the observed record long spin period of accreting magnetized NS. Note here that in this regime in the limit of vanishing accretion rate the NS still continues spinning-down by transferring angular momentum through the magnetospheric plasma shell, to eventually reach the orbital period of the binary system,  $P_{eq}^*|_{\dot{M} \rightarrow 0} \rightarrow P_b$ . While technically challenging, even longer NS spin periods can be found in very faint Galactic X-ray binaries in future sensitive X-ray observations.

## 5 CONCLUSIONS

A periodicity was discovered in AX J1910.7+0917 during *Chandra* observations that serendipitously covered the source region (Israel et al. 2016, see also Section 3.2). Since AX J1910.7+0917 is identified with a HMXB hosting a massive B-type star, the coherent signal at 36.2 ks can be explained only as the rotational period of the NS. This discovery makes AX J1910.7+0917 the pulsar with the slowest spin period. A quasi-spherical settling accretion model (Shakura et al. 2012) is able to explain this superslow pulsation, even adopting a typical NS surface magnetic field of  $\sim 10^{12}$  G. However, before a firm conclusion about the NS magnetic field can be drawn from the theory, other source parameters (orbital period, velocity of the wind outflowing from the massive donor) are needed. Future sensitive spectroscopy above 10 keV would also be desirable, to detect cyclotron resonant scattering features and obtain a direct measurement of the NS magnetic field in AX J1910.7+0917.

## ACKNOWLEDGMENTS

This work is based on data from observations with *XMM-Newton* and *Chandra*. *XMM-Newton* is an ESA science mission with instruments and contributions directly funded by ESA Member States and the USA (NASA). The scientific results reported in this article are also based on data obtained from the *Chandra* Data Archive. This research has made use of software provided by the *Chandra* X-ray Center (CXC) in the application package CIAO, and of the SIMBAD database, operated at CDS, Strasbourg, France. LS acknowledges the grant from PRIN-INAF 2014, “Towards a unified picture of accretion in High Mass X-Ray Binaries” (PI: L. Sidoli). LS and KP acknowledge support from the International Space Science Institute (Switzerland) during a team meeting held in Bern in 2017 (PI: S. Martínez-Núñez). KP also acknowledges partial support from RSF grant 16-12-10519 for travel to the ISSI meeting. PE acknowledges funding in the framework of the NWO Vidi award A.2320.0076 (PI: N. Rea).

## REFERENCES

Bird A. J., Bazzano A., Malizia A., Fionchi M., Sguera V., Bassani L., Hill A. B., Ubertini P., Winkler C., 2016, *ApJS*, 223, 15  
 Dall’Osso S., Israel G. L., Stella L., Possenti A., Perozzi E., 2003, *ApJ*, 599, 485  
 De Luca A., Caraveo P. A., Mereghetti S., Tiengo A., Bignami G. F., 2006, *Science*, 313, 814  
 Drave S. P., Clark D. J., Bird A. J., McBride V. A., Hill A. B., Sguera V., Scaringi S., Bazzano A., 2010, *MNRAS*, 409, 1220  
 Evans I. N., Primini F. A., Glotfelty K. J., Anderson C. S., Bonaventura, N. R., Chen J. C., Davis J. E., Doe S. M., Evans J. D., Fabbiano G., et al., 2010, *ApJS*, 189, 37  
 Finley J. P., Belloni T., Cassinelli J. P., 1992, *A&A*, 262, L25  
 Garmire G. P., Bautz M. W., Ford P. G., Nousek J. A., Ricker Jr. G. R., 2003, in Truemper J. E., Tananbaum H. D., eds, *X-Ray and Gamma-Ray Telescopes and Instruments for Astronomy*. Vol. 4851 of Proceedings of the SPIE., Advanced CCD imaging spectrometer (ACIS) instrument on the Chandra X-ray Observatory. pp 28–44  
 Grundstrom E. D., Blair J. L., Gies D. R., Huang W., McSwain M. V., Raghavan D., Riddle R. L., Subasavage J. P., Wingert D. W., Levine A. M., Remillard R. A., 2007, *ApJ*, 656, 431

Hall T. A., Finley J. P., Corbet R. H. D., Thomas R. C., 2000, *ApJ*, 536, 450  
 Hu C.-P., Ng C.-Y., Chou Y., 2016, *Journal of Astronomy and Space Sciences*, 33, 173  
 Israel G. L., Esposito P., Rodríguez Castillo G. A., Sidoli L., 2016, *MNRAS*, 462, 4371  
 Leahy D. A., Darbro W., Elsner R. F., Weisskopf M. C., Kahn S., Sutherland P. G., Grindlay J. E., 1983, *ApJ*, 266, 160  
 Liu Q. Z., van Paradijs J., van den Heuvel E. P. J., 2006, *A&A*, 455, 1165  
 Lopez L. A., Ramirez-Ruiz E., Castro D., Pearson S., 2013, *ApJ*, 764, 50  
 Lucas P. W., Hoare M. G., Longmore A., Schröder A. C., Davis C. J., Adamson A., Bandyopadhyay R. M., de Grijs R., Smith M., Gosling A., Mitchison S., et al., 2008, *MNRAS*, 391, 136  
 Marcu D. M., Fürst F., Pottschmidt K., Grinberg V., Müller S., Wilms J., Postnov K. A., Corbet R. H. D., Markwardt C. B., Cadolle Bel M., 2011, *ApJL*, 742, L11  
 Martínez-Núñez, S., Kretschmar, P., Bozzo, E., et al. 2017, *ArXiv e-prints*, arXiv:1701.08618  
 Miceli M., Decourchelle A., Ballet J., Bocchino F., Hughes J. P., Hwang U., Petre R., 2006, *A&A*, 453, 567  
 Pavan L., Bozzo E., Ferrigno C., Ricci C., Manousakis A., Walter R., Stella L., 2011, *A&A*, 526, A122  
 Rodes-Roca J. J., Torrejón J. M., Martínez-Núñez S., Bernabéu G., Magazzú A., 2013, *A&A*, 555, A115  
 Shakura N., Postnov K., 2017, *ArXiv e-prints*  
 Shakura N., Postnov K., Kochetkova A., Hjalmarsdotter L., 2012, *MNRAS*, 420, 216  
 Shakura N., Postnov K., Sidoli L., Paizis A., 2014, *MNRAS*, 442, 2325  
 Sidoli L., Romano P., Mereghetti S., Paizis A., Vercellone S., Mangano V., Götz D., 2007, *A&A*, 476, 1307  
 Strüder L., Briel U., Dennerl K., Hartmann R., Kendziorra E., Meidinger N., Pfeffermann E., Reppin C., et al. 2001, *A&A*, 365, L18  
 Sugizaki M., Mitsuda K., Kaneda H., Matsuzaki K., Yamauchi S., Koyama K., 2001, *ApJS*, 134, 77  
 Turner M. J. L., Abbey A., Arnaud M., Balasini M., Barbera M., Belsole E., Bennie P. J., Bernard J. P., et al. 2001, *A&A*, 365, L27  
 Verner D. A., Ferland G. J., Korista K. T., Yakovlev D. G., 1996, *ApJ*, 465, 487  
 Walter R., Lutovinov A. A., Bozzo E., Tsygankov S. S., 2015, *A&A Rev.*, 23, 2  
 Wilms J., Allen A., McCray R., 2000, *ApJ*, 542, 914

This paper has been typeset from a  $\text{\TeX}/\text{\LaTeX}$  file prepared by the author.